Appl. Phys. B 68, 45–53 (1999)

Applied Physics B
Lasers
and Optics

Dynamics and correlated performance of a photo-triggered discharge-pumped HF laser using SF_6 with hydrogen or ethane

L. Richeboeuf, S. Pasquiers, F. Doussiet, M. Legentil, C. Postel, V. Puech

Laboratoire de Physique des Gaz et des Plasmas (associé au CNRS), Université Paris XI, Bât.212, 91405 Orsay Cedex, France
(E-mail: Stephane.Pasquiers@lpgp.u-psud.fr)

Received: 17 March 1998/Revised version: 13 July 1998

Abstract. A detailed experimental study of an X-ray photo-triggered HF laser, with an active volume of 312 cm^3, has been performed in $Ne/SF_6/H_2$ and $Ne/SF_6/C_2H_6$ mixtures. Parameters involved have been the storage line capacitance and the circuit inductance, the capacitors charging voltage, the RH-molecule type and partial pressure, and the X-ray dose for the preionization. High laser performance has been achieved with C_2H_6: an output energy up to 3 J corresponding to a specific energy of 9.6 J/l at an efficiency of 4.7%, which strengthens the advantage of the photo-triggering technique to energize high-power HF lasers. However the optimum performance achieved with H_2, 5.75 J/l and 3.5%, are lower. It is shown, through a time-resolved study of the electrical discharge and spatial dynamics correlated to laser power and energy measurements, that discharge instabilities are responsible for the poor laser performance of the mixture with H_2. These instabilities, which lead to arc development, are characteristics of the discharge in Ne/SF_6. It is demonstrated for the first time that addition of a heavy hydrocarbon, such as C_2H_6, to that mixture induces the discharge stabilization so that the laser emission arises in a homogeneous active medium. This effect allows us to achieve better laser performance than with H_2.

PACS: 42.55.Ks; 52.80.-s

Discharge-pumped non-chain HF/DF chemical lasers have been widely studied since 1967 [1–21]. These lasers are much easier to handle than those using H_2/F_2 chain reaction mixtures, as the rovibrational levels of the HF molecule are produced by reaction between a hydrogenated compound RH and the F atoms obtained from the dissociation of a chemically inert molecule. It has been recognized early that SF_6 allows us to achieve the highest laser performance, i.e. output energy and electrical efficiency, rather than the performance obtained with other molecules such as fluorocarbons [2, 4]. Moreover it is well known, from the work by Voignier and Gastaud [7], that the most efficient discharge type to energise SF_6/RH active media is the preionized transverse discharge between adequately profiled electrodes. Preionizers such as semiconductors [12], corona or sliding discharges [9–11, 13, 15–17] (UV photons), or cold-cathode diode [14, 18–21] (X-rays), have been employed with various discharge operation techniques. Amongst these techniques, the photo-triggering has allowed us to obtain the best performance achieved up to now for the discharge-pumped non-chain HF laser, i.e. the highest specific energy at the highest electrical efficiency [13–15, 18]. Using the photo-triggering with UV-corona preionization, and for an active volume of 1.4 litres, Brunet et al. [15] have obtained a laser energy up to 12 J per pulse, which gives a specific energy of 8.6 J/l. This energy has been achieved at an overall efficiency of 3%, with a three-component mixture of Ne, SF_6, and C_2H_6. Moreover, with same gases, a specific energy up to 11 J/l at an efficiency higher than 3% has been reached with a small X-ray preionized laser (50 cm^3), named X510 [14]. With the same type of preionization, we have recently reported preliminary results on a 312-cm^3 laser [18], X525, which strengthen the view that the active volume can be increased without loss of performance: 9.6 J/l has been obtained at an efficiency of 4.7%.

In the photo-triggered scheme, the discharge electrodes are directly connected to an energy storage unit charged up to a voltage V_o in a few μs. Once the desired voltage has been reached, the preionization is achieved by means of UV photons or X-rays and initiates the gas breakdown with a variable time lag. The voltage V_o must be chosen so that the initial reduced electric field $(E/N)_o$, i.e. the field applied across the electrodes at the time of the preionization, is higher than the self-sustaining electric field of the discharge in the gas mixture used; $(E/N)_o$ is defined by: $(E/N)_o = V_o/(Nd)$, where N is the total mixture density and d is the inter-electrode gap. The photo-triggering has already been proved very efficient for energizing a gas mixture that contains an important concentration of strongly electronegative molecules [13, 18, 21, 22]. Indeed, as the initial field $(E/N)_o$ is higher than the self-sustaining field, the electrons obtained from the preionization are quite rapidly multiplied at an ionization rate higher than

the loss rate by attachment, which is favourable for the development of a homogeneous discharge on condition that the initial electron density is high enough. As described above, this concept has been successfully applied to the HF laser using SF_6 as F-atom donor. However such a success has been obtained using ethane instead of hydrogen to react with F, as the specific energy and the efficiency achieved with $RH = H_2$ are lower than with $RH = C_2H_6$. Typically, with hydrogen, 7 J/l at 1.8% is achieved with the X510 laser [14], and 5.75 J/l at 3.1% with the X525 laser [18].

The improvement of the laser performance as hydrogen is replaced by a heavy hydrocarbon, i.e. with at least two carbon atoms, has been discovered since the first studies on discharge-pumped HF lasers [2, 4]. It has been established with all discharge devices studied up to now, from pin electrodes [4] to continuous profiled ones [14], but no clear explanation for this effect has been proposed. In a recent paper on the photo-triggered HF laser [21], we have demonstrated that the higher laser performance obtained with C_2H_6, compared with the performance obtained with H_2, cannot be explained in terms of different electrical energy and charge transmitted to the plasma, and of different F-atom production kinetics. However these results hold for a homogeneous active medium. A detailed comparison between the discharge spatial dynamic in mixtures of SF_6 with H_2 or SF_6 with C_2H_6 using the same discharge device, and the implication for the laser performance that could be achieved with such mixtures, has not been yet reported. Thus we have performed an investigation of the X-ray photo-triggered HF laser for both $Ne/SF_6/H_2$ and $Ne/SF_6/C_2H_6$ mixtures, over a large range of values of parameters such as the partial pressure of the RH molecule, or the initial applied voltage. The dependence of the photo-triggered laser behaviour and performance on the electrical circuit configuration, i.e. the storage line capacitance and the circuit inductance has been also examined. For this purpose, time-resolved current and voltage measurements have been performed together with the measure of the laser energy and of the temporal evolution of the laser power. These diagnostics have been coupled to examination of the active medium homogeneity through spatially and temporally resolved measurements of the plasma fluorescence intensity in the inter-electrode space.

The following part presents the experimental setup and diagnostics. The photo-triggered HF laser is characterized for low storage capacitance and low circuit inductance values in Sect. 2. The dependence on the circuit configuration is discussed in Sect. 3, through the increase of the capacitance and of the inductance. Conclusions are given in Sect. 4.

1 Experimental setup and diagnostics

1.1 General features

A cross-sectional view of the experimental structure, called "X525", is given in Fig. 1. It is a compact design already used to energize the XeCl* (308 nm) excimer laser [23]. The energy storage unit is made of ceramic capacitors placed in four-stage symmetric plate holders, with a total capacitance C ranging from 72 nF up to 144 nF. The charging voltage V_o can be chosen as high as 35 kV. The value of the total circuit inductance L depends on the geometrical configuration of the

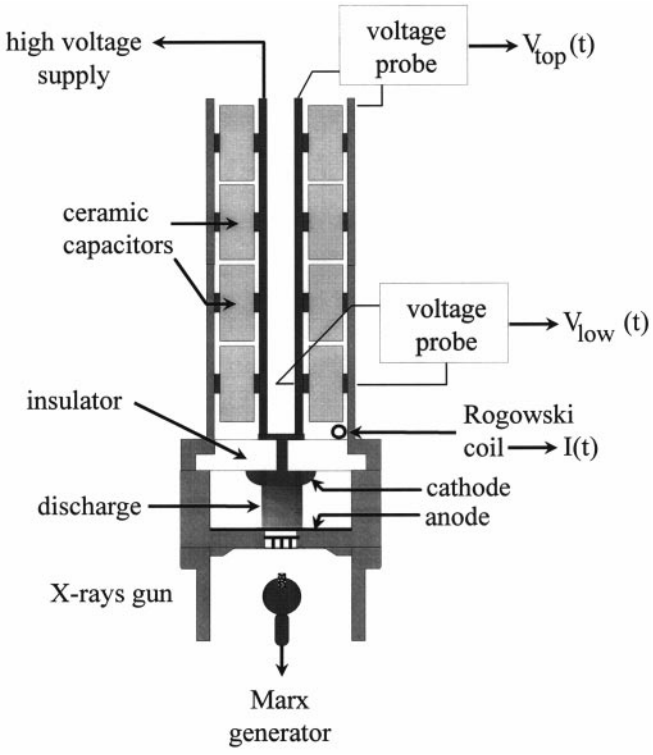

Fig. 1. Cross-sectional view of the X525 photo-triggered laser

capacitors. The inductance between each capacitor stage has been estimated to be 2 nH, and the one for the discharge cell is 9.25 nH. Thus L ranges from 11.25 nH, which corresponds to $C = 72$ nF with two capacitor stages in the lower positions, up to 15.25 nH, which corresponds to $C = 144$ nF with a full storage unit.

The upper electrode, which is 50 cm long and has a flat profile over 2.5 cm width, is the cathode. The inter-electrode gap, 2.5 cm, is controlled with a precision better than 1%, which ensures quite good spatial uniformity of the applied electric field. The preionization is achieved by a short (12 ns) X-ray burst generated from a cold-cathode diode powered by a low-inductance Marx generator. The X-rays enter the cell through the flat earthen electrode. The X-ray dose is fixed at 10 mrad.

The discharge cell has been filled with neon and SF_6 at the same concentration (1/1) at a total pressure of 118 Torr, with addition of hydrogen or ethane at a partial pressure p_{RH} ranging from 2 up to 22 Torr. A weak gas flow has been set in order to eliminate the ground-state HF molecules in a zeolite trap between each laser shot. Mixtures with H_2 or C_2H_6 will be called H_2 mixtures or C_2H_6 mixtures in the following.

1.2 Electrical diagnostics

The voltage across the capacitors has been measured using classical high-impedance probes (Tektronix 6015). On the other hand the current has been measured using a home-made linear self-integrated Rogowsky coil, which can be inserted between the capacitor bank and the upper discharge electrode without increasing the circuit inductance [24]. An example of electrical measurements is given in Fig. 2 for $C = 144$ nF, for

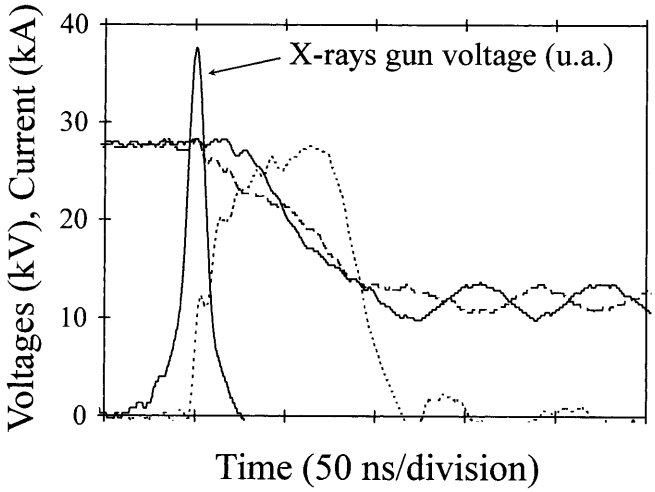

Fig. 2. Temporal evolutions of the current *(dotted line)*, upper voltage *(full line)*, and lower voltage *(dashed line)*, together with the X-ray gun voltage waveform. Mixture with ethane at 15 Torr partial pressure. $C = 144$ nF. $V_o = 28$ kV

the C_2H_6 mixture at 15 Torr of ethane, and for $V_o = 28$ kV. The temporal evolution of the voltages at the top of the capacitor holders, V_{top}, and across the lowest capacitor stage, V_{low}, are shown together with the current. The X-ray gun voltage waveform indicates the preionization time. For the operating conditions of the photo-triggered HF laser, the time delay between the preionization and the discharge breakdown is very short. The voltage V_{low} begins to drop, and the current develops, just at the time of the X-ray generation. The drop of the voltage V_{top} is delayed owing to the inductance distribution along the storage line. The discharge is characterized by a single current pulse. The current rises to its peak value I_c in 70 ns, and then decreases to zero in 55 ns. For $C = 72$ nF, we obtain a symmetric current waveform with a duration of 85 ns. In such cases the energy transmitted to the discharge, E_{trans}, is given by:

$$E_{trans} = \frac{C}{2}V_o^2 - \frac{C}{2}V_{res}^2 = E_{sto} - \frac{C}{2}V_{res}^2 ,$$

where E_{sto} is the initially stored energy and V_{res} is the residual voltage after the current pulse. The transmitted charge, Q_{trans}, is given by $Q_{trans} = C(V_o - V_{res})$. The residual voltage is particular to a discharge in a gas mixture that contains a strong electronegative component [13, 21, 22]. Such a feature reflects the competition between electron losses by attachment and electron production by ionization processes during the discharge.

1.3 Optical diagnostics

The optical cavity comprises a total reflector and a CaF_2 window. The laser energy is measured with a Gentec ED500 joulemeter and the temporal shape of the laser power is monitored with a Ge-Au detector. Absolute value of the power is obtained by normalization of the integrated detector signal against the measured energy.

A Hamamatsu CCD camera, equipped with a high-speed gated image intensifier, has been implemented on the laser

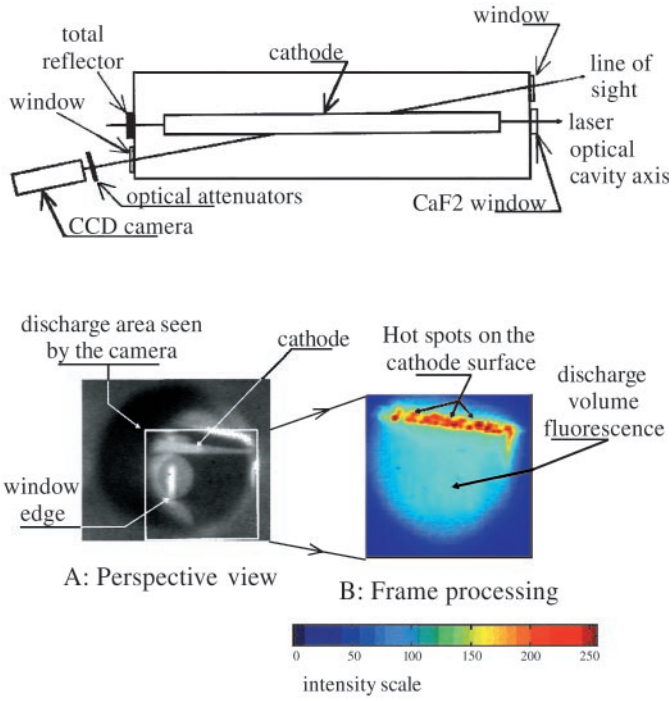

Fig. 3. Setup for the measurement of the plasma fluorescence in the inter-electrode space. Upper diagram: top view of the discharge cell. Frame A: cell inside seen by the CCD camera. Frame B: example of processing of the fluorescence intensity in pseudo-colours, for a homogeneous discharge in neon

structure as described in Fig. 3. It measures the plasma fluorescence intensity in the visible wavelength range, and is placed on a line of sight making a small angle with the optical cavity axis. The discharge cell inside seen by the camera is shown on the frame A. The cathode, located at the top of the frame, is seen in perspective on more than three quarters of its length. Frame B gives an example of intensity measurement, processed in pseudo-colours, for a discharge in pure neon. The light intensity scale ranges from dark blue, which corresponds to areas where there is no plasma fluorescence, to red which corresponds to saturation of the detector. The intensity can be reduced by neutral attenuators, and the exposure time has been fixed at 20 ns. Only the discharge space, delimited by a white square in frame A, is shown in frame B, as well as in all other frames of the present paper. An intense light emission arises from the cathode in frame B. Hot spots are distributed all along the electrode length. The volume fluorescence, less intense, is also homogeneous. These features are characteristics of a spatially homogeneous distribution of current density.

2 Laser characterization at low capacitance

2.1 Output energy and overall efficiency

In Fig. 4 the laser energy E_L at $C = 72$ nF for the C_2H_6 and H_2 mixtures is plotted against the stored energy E_{sto}. For each RH-pressure value, the stored energy threshold for the laser emission, E_{oth}, corresponds to the voltage threshold V_{oth} determined by the critical field $(E/N)_{oc}$ at which electron

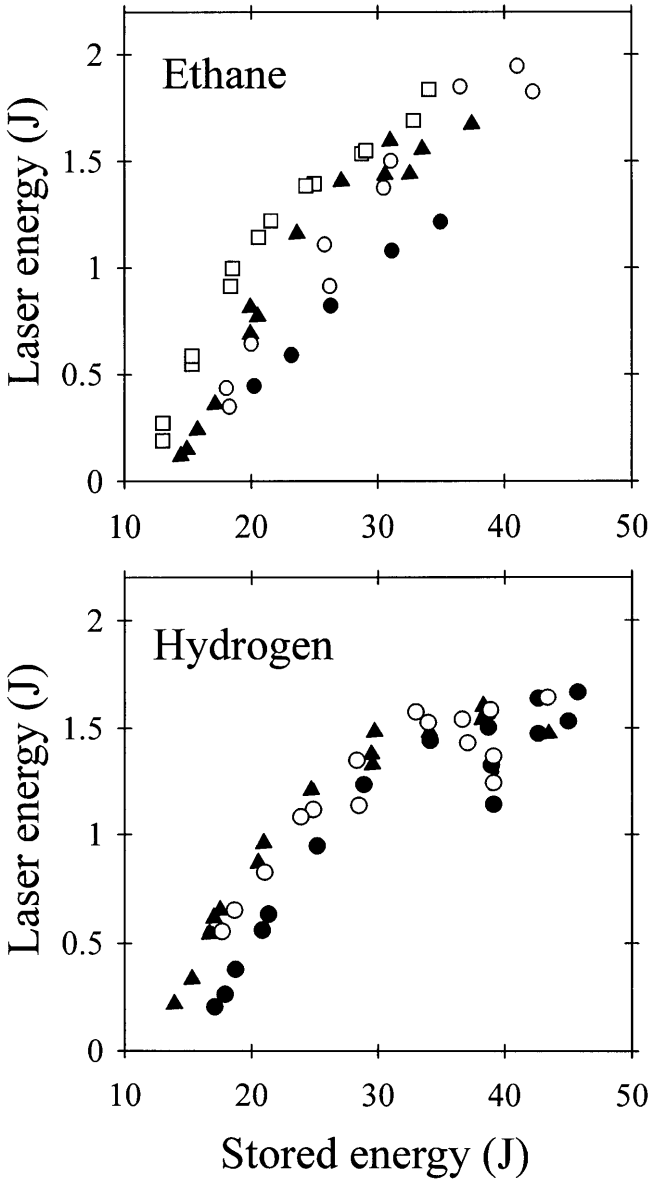

Fig. 4. Laser energy plotted against the initially stored electrical energy, for mixtures with ethane *(upper diagram)* and with hydrogen *(lower diagram)* at $C = 72$ nF. RH partial pressure: (□)2 Torr, (▲)7.5 Torr, (○)11.5 Torr, (●)22 Torr

production and loss rates are equal. The discharge develops for $(E/N)_o$ higher than $(E/N)_{oc}$.

Figure 4 shows that the laser energy is an increasing function of the stored energy at all ethane pressures, i.e. 2, 7.5, 11.5, and 22 Torr. At a fixed C_2H_6 pressure, examination of the overall efficiency η, defined by $\eta = E_L/E_{sto}$, emphasizes that η rapidly increases as E_{sto} increases from E_{oth} up to a value above which η slightly decreases. Moreover, at a given E_{sto} value, the laser energy and efficiency decrease when the ethane pressure increases. Hence the maximum η value obtained at 22 Torr is 3.5%, whereas it is about 6% at 2 Torr.

At a low stored energy, from E_{oth} up to about 30 J, the evolution of the laser energy and of the efficiency obtained for the H_2 mixture, against E_{sto}, are qualitatively identical to those obtained for the C_2H_6 mixture. However, E_L saturates as E_{sto} increases above 30 J in the case of hydrogen, in contrast to the case of ethane, with important fluctuation of the laser energy measured from one shot to another. This effect is encountered at all p_{RH} values studied. Thus, in the H_2 mixture, the efficiency rapidly decreases when E_{sto} increases above 30 J.

2.2 Discharge dynamics and effect on laser emission

Figures 5a and 5b show measurements on the discharge dynamics and on the laser power for the H_2 mixture at $C = 72$ nF. Results are given for two consecutive discharges at $p_{RH} = 7.5$ Torr and $V_o = 28.35$ kV, i.e. $E_{sto} = 29$ J. The temporal evolution of the voltage V_{top} and of the current are plotted for each discharge. The temporal evolution of the laser power, which arises at the end of the discharge, is given for the first one. Frames denoted 1 and 2 in Fig. 5b have been obtained at the same time for the camera opening, whose signal is plotted in the upper diagram in Fig. 5a. This time corresponds to the time of the laser peak power for the conditions of the figure.

Except for a charging voltage value very close to the threshold value V_{oth}, the discharge behaviour is identical to the example given in the upper diagram in Fig. 5a for all V_o values lower than 28 kV at $p_{RH} = 7.5$ Torr. The plasma volume fluorescence is homogeneous during the current pulse, and a residual voltage V_{res} is established after the discharge. One or several arcs can appeared, but at a time of several μs. In that case a few cathodic spots are detected at the end of the voltage drop as illustrated in frame 1, but examination of the fluorescence at later times shows that the cathodic emission intensity decreases during the voltage plateau. The laser emission arises in a medium which presents no spatial inhomogeneity in the discharge volume, and the laser energy is reproducible from one shot to another.

On the other hand, at a charging voltage higher than 28 kV at 7.5 Torr of hydrogen, the laser behaviour is not shot-to-shot reproducible as shown in Fig. 5a and 5b, for which V_o is just a little higher than 28 kV. In that case the discharge is alternatively, from shot to shot, homogeneous (first discharge, frame 1) or inhomogeneous (second discharge, frame 2) at the end of the current pulse. A second current pulse is measured in the lower diagram in Fig. 5a, whose waveform is not reproducible, and the fluorescence measurement during this pulse shows localized intense filaments. Frame 2 shows that appearance of these filaments is correlated to the development of some of the cathodic spots. It reveals a discharge instability onset before the end of the first current pulse, which is characterized by the development of an inhomogeneous distribution of current density. Correlatively the laser energy achieved with the second discharge is about 20% lower than the energy obtained with the first one, although all parameter values are identical for the two discharges. For V_o well above 28 kV, the duration of the residual voltage plateau is reduced to a few tenths of ns, and the discharge is always non-uniform with the presence of bright filaments during the laser emission.

We have established that addition of H_2 to the binary $Ne/SF_6(1/1)$ mixture has little influence on the discharge dynamic. Plasma inhomogeneities appear at all H_2 pressure studied, and similar measurements to those shown in Fig. 5 have been obtained for discharges in $Ne/SF_6(1/1)$. The only effect of H_2 addition is the increase of the threshold charg-

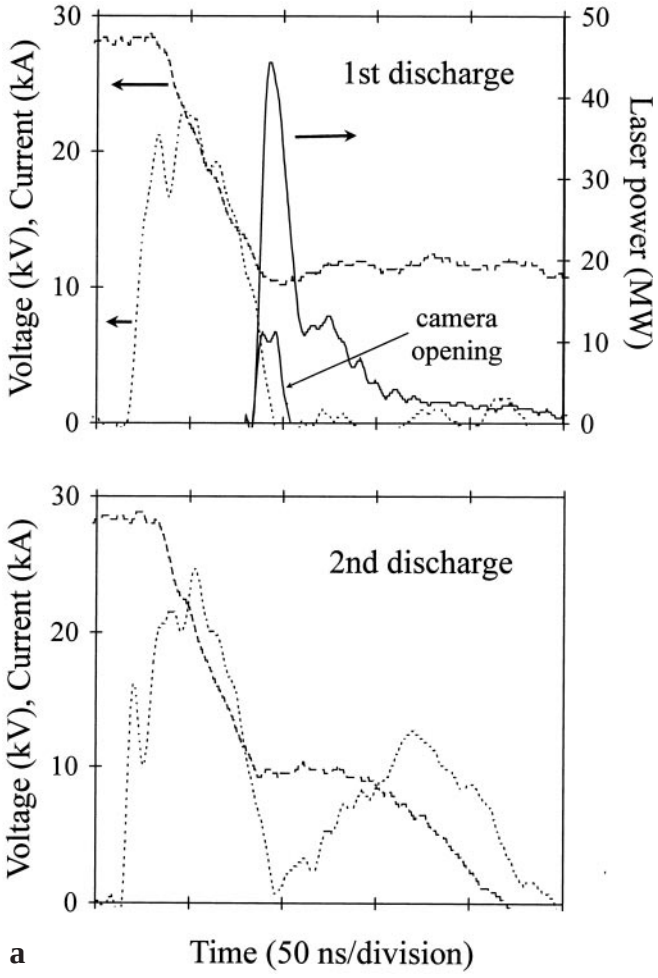

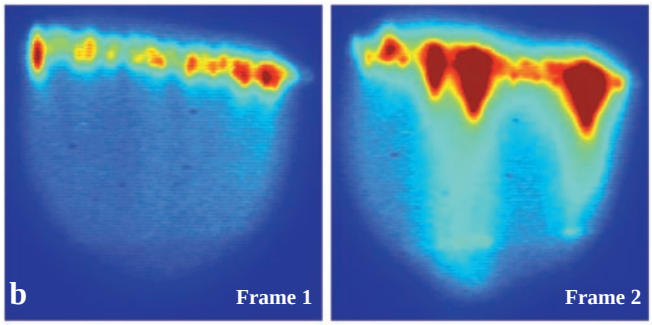

Fig. 5. a Temporal evolutions of the current *(dotted line)*, upper voltage *(dashed line)*, and laser power (*full line* in the *upper diagram*) for the mixture with hydrogen at 7.5 Torr partial pressure, for two consecutive discharges at $C = 72$ nF and $V_o = 28.35$ kV. Measured laser energy values: first discharge 1.4 J; second discharge 1.15 J. The signal for the camera opening, whose corresponding frames are displayed in Fig. 5b, is shown in the upper diagram. **b** Fluorescence measurements in the conditions of Fig. 5a: frames 1 (first discharge) and 2 (second discharge) have been obtained at the same time for the camera opening (time of the laser peak power). Optical attenuation for both frames: 2.75 dB

ing voltage value for the instability onset, V_{ons}, as p_{RH} increases. $V_{ons} = 28$ kV at $p_{RH} = 7.5$ Torr, and $V_{ons} = 30.5$ kV at $p_{RH} = 22$ Torr. It corresponds to an initial reduced field equal to 271 Td and 265 Td, respectively. Hence instabilities appear at a roughly constant $(E/N)_o$ value.

Thus, as a result of the instability onset in the H_2 mixture, the laser energy saturates and the efficiency decreases when E_{sto} increases above 30 J, Fig. 4. In contrast, no instability has been observed in the C_2H_6 mixture at $C = 72$ nF, in the whole range of charging voltage and ethane pressure values studied. The discharge behaviour and the laser energy are very reproducible from shot to shot. As for the H_2 mixture a high-intensity cathodic emission is detected, but none of the hot spots develops in the discharge volume and the discharge quality appears as good as in Fig. 3. No arc occurs at the end of the current pulse. Correlatively the laser energy continuously increases when the stored energy increases, Fig. 4, without saturation effect. In fact the addition of C_2H_6 to $Ne/SF_6(1/1)$ induces the stabilization of the discharge, and thus the homogenization of the active medium. This effect arises even at low ethane concentration in the mixture, 1.6% at a low capacitance $C = 72$ nF.

2.3 Energy deposition and intrinsic efficiency of the homogeneous medium

The energy deposition, which is characterized by the transmission efficiency η_{trans}, defined by $\eta_{trans} = E_{trans}/E_{sto}$, can be readily optimized to 100% in the case of ethane, without loss of discharge homogeneity. This is obtained by choosing V_o so that $V_{res} = 0$, which is achievable for a charging voltage of at least a factor two higher than the discharge threshold value V_{oth}. Such an optimization is much more difficult to perform in the case of hydrogen, because part of the initially stored energy is transmitted into arcs when V_o increases above V_{ons}. However, at V_o less than V_{ons}, it is noted that the charge and energy deposition in the medium is about the same for the H_2 and C_2H_6 mixtures. It results from the electron kinetics in these mixtures [21].

On the other hand, it is known that the increase of the transmitted charge, and energy, leads to the increase of the total fluorine atom density produced in the discharge, $[F]_{prod}$. Moreover, $[F]_{prod}$ decreases when H_2 is replaced by C_2H_6 at a high p_{RH} value [21]. Consequences are twofold for a homogeneous medium. First, a continuous increase of the laser energy E_L is readily achieved at a fixed p_{RH} value, Fig. 4 (E_{sto} less than 30 J), by the increase of Q_{trans} and E_{trans}, which is obtained from the increase of V_o, i.e. the increase of $(E/N)_o$. At a low RH partial pressure, the $[F]_{prod}$ value is quasi-identical in the H_2 and C_2H_6 mixtures so that the corresponding laser energy and efficiency values are very little different. Second, at a fixed E_{trans} value, the laser energy obtained with C_2H_6 decreases more rapidly when p_{RH} increases, than E_L obtained with H_2. This is illustrated in Fig. 6, in which is plotted the intrinsic efficiency of the medium, η_{int}, defined by $\eta_{int} = E_L/E_{trans}$, against the transmitted energy at $p_{RH} = 7.5$ and 22 Torr. At a low pressure, 7.5 Torr, η_{int} is identical for the H_2 and C_2H_6 mixtures. However, at 22 Torr, the intrinsic efficiency is lower for the C_2H_6 mixture than for the H_2 one. For that pressure value, the difference between $\eta_{int}(H_2)$ and $\eta_{int}(C_2H_6)$ is about 1%, in absolute value, on the whole range of transmitted energy values studied. In addition, quenching of the HF rovibrational levels by C_2H_6, through v-v and v-T processes [25], could also contribute to the decrease of E_L and η when the ethane pressure increases.

Both for H_2 and C_2H_6 mixtures, η_{int} decreases when E_{trans} increases at a fixed p_{RH} value, Fig. 6. As a result η, which is

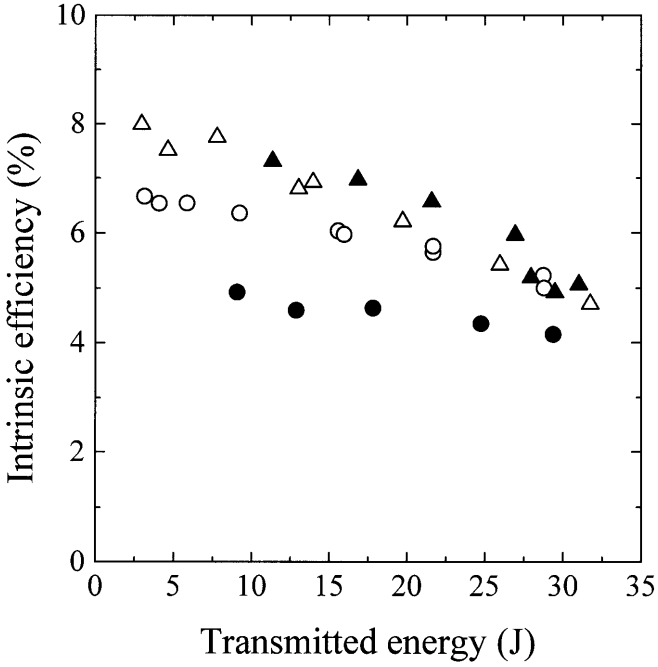

Fig. 6. Intrinsic efficiency of the active medium plotted against the transmitted energy for mixtures with hydrogen or ethane, at $C = 72$ nF. Hydrogen partial pressure: (△)7.5 Torr, (○)22 Torr; Ethane partial pressure: (▲)7.5 Torr, (●)22 Torr

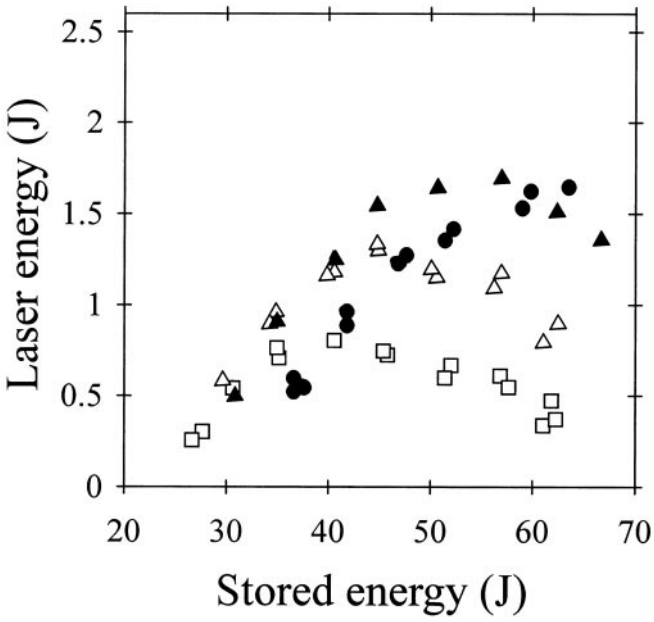

Fig. 7. Laser energy plotted against the initially stored electrical energy, for mixtures with hydrogen at $C = 144$ nF. Hydrogen partial pressure: (□)2 Torr, (△)4 Torr, (▲)7.5 Torr, (●)22 Torr

simply equal to the product $\eta_{\text{trans}}\,\eta_{\text{int}}$, saturates and slightly decreases, in the case of ethane, when E_{sto} increases. This saturation also occurs in the case of hydrogen, but it is rapidly dominated by the effect of discharge instabilities as soon as E_{sto} is higher than 30 J.

3 Dependence on circuit configuration

Interest in the increase of the storage capacitance, as far as a factor two higher than the configuration studied in the previous section, is to determine if the laser performance achieved with H_2 and C_2H_6 mixtures can be improved through the increase of the charge and energy transmitted to the active medium, without enhancement of the initial field $(E/N)_o$ above the critical value, 265 Td, established for the instability onset at $C = 72$ nF. In the present work the total inductance L has also been increased owing to the increase of the geometrical dimensions of the energy storage unit as the number of capacitors increases. It leads to the increase of the discharge duration of about 40 ns.

3.1 Gas mixtures with hydrogen

3.1.1 Laser performance. For the H_2 mixture, the laser energy E_L measured at $C = 144$ nF is plotted in Fig. 7 against the stored energy E_{sto}, at $p_{RH} = 2$, 4, 7.5, and 22 Torr. At all p_{RH} values studied, the laser threshold value E_{oth} is a factor two higher than in Fig. 4 owing to the doubling of the capacitance. At E_{sto} slightly higher than E_{oth}, the evolution of E_L as p_{RH} or E_{sto} vary is nearly the same as at $C = 72$ nF. However a strong saturation effect is seen on E_L values when E_{sto} increases well above the threshold. At a given H_2 pressure, the laser energy and the efficiency η reach maximum values at critical stored energy values, E_{sc}, which depend on p_{RH}. For the laser energy, E_{sc} increases from 40 J at 2 Torr, up to 55 J at 15 Torr, Fig. 7. Both E_L and η decrease as E_{sto} increases above the critical values, at p_{RH} lower than 15 Torr. At a given low stored energy, below 35 J, the laser energy and the efficiency weakly depend on the H_2 pressure at p_{RH} less than 10 Torr. In contrast, at a stored energy higher than 45 J, E_L and η rapidly increase when p_{RH} increases from 2 up to 7.5 Torr. However, in that range of E_{sto} values, E_L and η weakly depend on the H_2 pressure for p_{RH} between 7.5 and 22 Torr. It should be observed that E_{sc} has not been reached at 22 Torr, but E_L clearly begins to saturate when E_{sto} increases above 55 J. For that high pressure value, the efficiency is constant and equal to 2.65% at E_{sto} higher than 45 J.

As a result of the parametric study, the maximum laser energy achieved at $C = 144$ nF is $E_L = 1.8$ J at an efficiency $\eta = 3.1\%$ [18]. These E_L and η values are quasi-identical to the performance achieved at $C = 72$ nF. Thus the increase of the capacitance does not lead to an improvement of the laser performance for the H_2 mixture. The specific output energy and the overall efficiency are limited to 5.75 J/l and 3.5%, respectively, for the X525 laser, in the range of H_2 pressure values studied. Examination of the discharge dynamics coupled to the laser power measurement gives clear answers to these limitations, as discussed below.

3.1.2 Discharge dynamics and implications for the laser power. At $p_{RH} = 4$ Torr, Fig. 8a shows the temporal evolutions of the current, of the voltage, and of the laser power at $C = 144$ nF and at three values of the charging voltage V_o : 20.5 kV, 25.05 kV, and 29.15 kV ($E_{\text{sto}} = 30.3$ J, 45.2 J, and 61.2 J). The maximum laser energy is achieved at $V_o = 25$ kV for that H_2 pressure value. Camera measurements at $V_o = 25.05$ kV (frame 1) and 29.15 kV (frame 2), both at

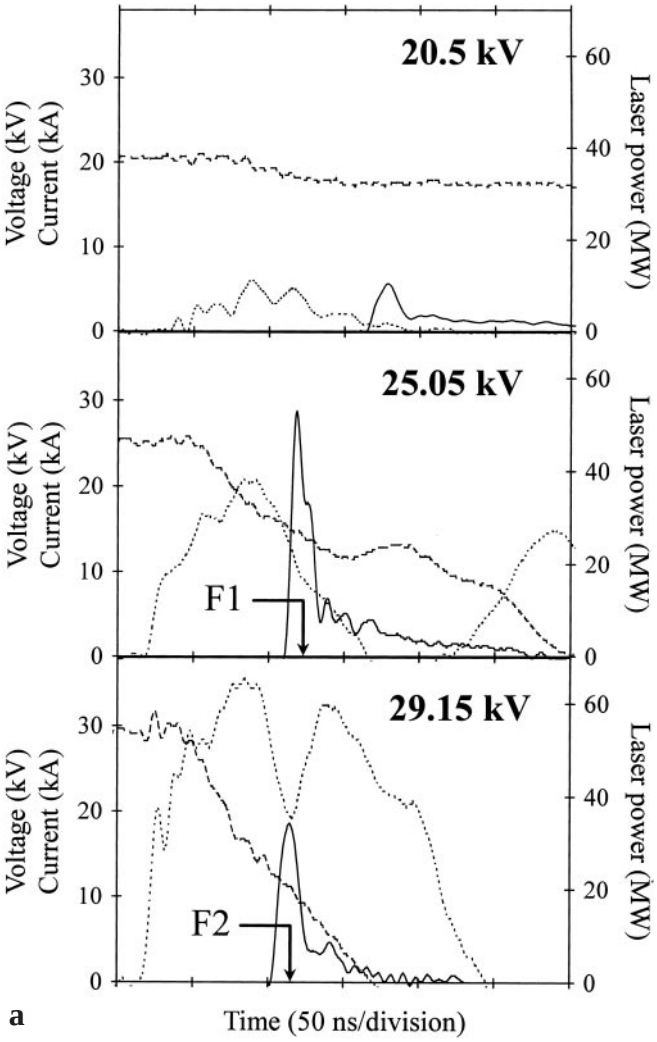

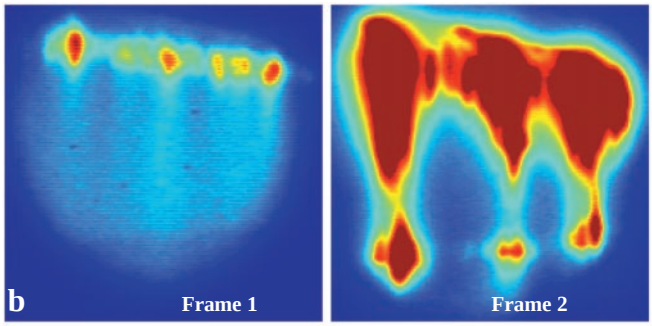

Fig. 8. a Temporal evolutions of the current (*dotted line*), upper voltage (*dashed line*), and laser power (*full line*) at $C = 144$ nF for the mixture with hydrogen at 4 Torr partial pressure. The initial applied voltage value is indicated on each diagram. Arrows in the medium and lower diagrams give locations of the camera opening for frames 1 and 2 in Fig. 8b. **b** Fluorescence measurements in the conditions of Fig. 8a. Optical attenuation: frame 1 – 4.75 dB; frame 2 – 7.5 dB

the time of the laser peak power (arrows in diagrams), are displayed in Fig. 8b.

At a low charging voltage value, the discharge current and voltage behaviours measured at $C = 144$ nF are of the same type as at $C = 72$ nF and V_o lower than 28 kV, as can be seen for $V_o = 20.5$ kV in Fig. 8a. The discharge is homogeneous. However a second current pulse, evidence of an instability, is measured close to the main discharge as V_o increases just a few kV above the discharge threshold voltage V_{oth}. In that condition, from shot to shot, the statistical delay time between the first peak current I_c and the second current pulse is, at maximum, a few times the discharge duration. This is not the case at $C = 72$ nF, for which the residual voltage remains across the electrodes during a time much higher than the discharge duration, for a charging voltage value up to at least $V_{oth} + 10$ kV. Thus the increase of C, from 72 nF up to 144 nF, induces a decrease of the threshold voltage V_{ons} for the instability onset.

At $V_o = 25$ kV and $C = 144$ nF, the delay time between I_c and the second current pulse is more or less equal to the discharge duration, 125 ns, Fig. 8a. The laser emission arises well before the instability onset at $p_{RH} = 4$ Torr, and frame 1 in Fig. 8b shows that the active medium is homogeneous at the time of the laser peak power P_c, with few hot spots on the cathode. However, the higher the charging voltage is above 25 kV, the shorter is the appearance time of the second current pulse with regard to the time of I_c. It means that the increase of V_o induces a rapid decrease of the delay time between P_c and the development of plasma inhomogeneities. At $V_o = 29.15$ kV, the instability appears when the current is about half of its maximum value, at less than 50 ns after the first peak current. In that condition, frame 2 in Fig. 8b shows that the maximum value of the laser power, which is less than the power at $V_o = 25$ kV, is achieved at a time for which strong plasma inhomogeneities have already developed. Measurement of the evolution of the peak power against the charging voltage shows that P_c first increases when V_o increases up to 25 kV, and thereafter decreases for higher V_o values. It explains the saturation and the decrease of the laser energy as E_{sto} increases above E_{sc}, Fig. 7.

As a result of the rapid development of plasma inhomogeneities when V_o increases, the H_2 pressure value takes a prominent part in the optimization of the laser performance. For instance, at $V_o = 29.4$ kV, $C = 144$ nF, and $p_{RH} = 2$ Torr, the peak power P_c is reached during the second current pulse and is only about 20 MW. For the same values of V_o and C, but at $p_{RH} = 7.5$ Torr, the laser emission begins to growth very close to the first peak current, and $P_c = 70$ MW. It reflects, at 7.5 Torr, a lesser influence of the instability on the laser emission than at 2 Torr. Thus the maximum laser energy achieved at 7.5 Torr is a factor of 2 higher than the energy obtained at 2 Torr, Fig. 7. However discharge instabilities prevent the achievement of a better laser performance at $C = 144$ nF than at 72 nF.

3.1.3 Parameters involved in discharge instabilities. Several parameters could take a part in the instability onset in Ne/SF_6, and thus in H_2 mixtures. Comparison between results obtained, for the X525 laser, at $C = 72$ nF and at $C = 144$ nF indicates that the temporal shape of the current pulse, the duration of this pulse, and the charge transmitted to the medium are amongst those parameters. In particular, the inhomogeneous second current pulse detected at 144 nF appeared at a transmitted charge value less than Q_{trans} measured at the threshold $(E/N)_o$ value for the instability onset at 72 nF. However the main discharge duration at 144 nF ($L = 15.25$ nH) is 40 ns higher than at 72 nF ($L = 11.25$ nH).

Work is in progress to determine the correlation, for the development of inhomogeneities, between the discharge duration and the transmitted charge, as well as to examine the influence of the cathode shape and of the SF_6 concentration in the mixture.

3.2 Gas mixtures with ethane

At $C = 144$ nF, the stabilization of the discharge due to the substitution of H_2 by C_2H_6 is illustrated in Fig. 9, which gives results obtained at $p_{RH} = 7.5$ Torr and $V_o = 28$ kV. Frames 1A and 1B, which correspond to the same time but for different optical attenuation values, emphasise that the laser peak power is achieved in a homogeneous medium, and that the cathodic luminescence is homogeneously distributed along the electrode length without significant spatial gradient of intensity. Some cathodic spots remain intense at the end of the discharge, frame 2, but no plasma filamentation develops and the residual voltage V_{res} is established in a time much higher than the current pulse duration, as for $C = 72$ nF. Thus, the increase of C leads to the increase of the transmitted charge and energy without significant deterioration of the spatial quality of the active medium. Moreover the transmission efficiency η_{trans} does not depend on the circuit configuration.

Consequences on the laser performance are given in Fig. 10, in which is displayed the evolution of the laser energy E_L against the stored energy E_{sto}, at $p_{RH} = 2$, 7.5, 15, and 22 Torr. Figures 7–10 clearly demonstrate, for the first time, that the laser performances achieved with ethane are higher

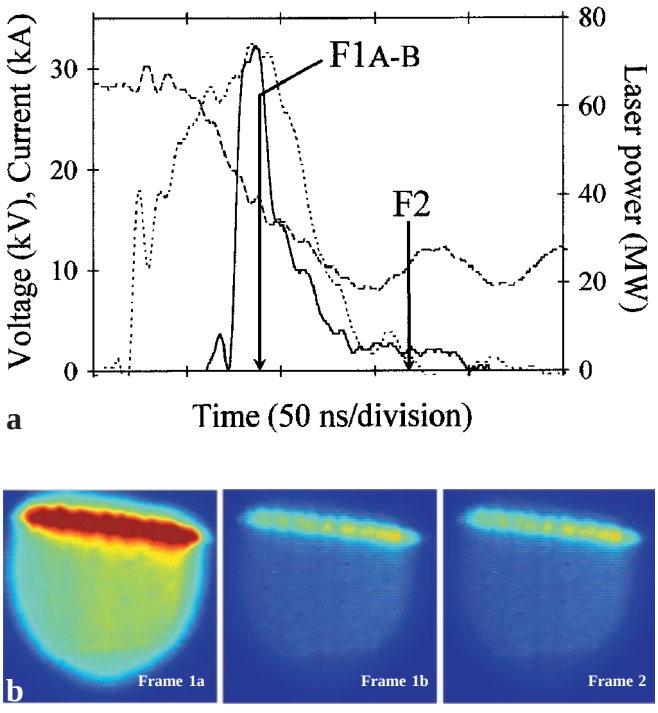

Fig. 9. Temporal evolutions of the current (*dotted line*), upper voltage (*dashed line*), and laser power (*full line*) for the mixture with ethane at 7.5 Torr partial pressure, at $C = 144$ nF and $V_o = 28$ kV, together with fluorescence measurements. Arrows show locations of the camera opening for frames 1A, 1B, and 2. Optical attenuation: frame 1A – none; frame 1B – 4.75 dB; frame 2 – none

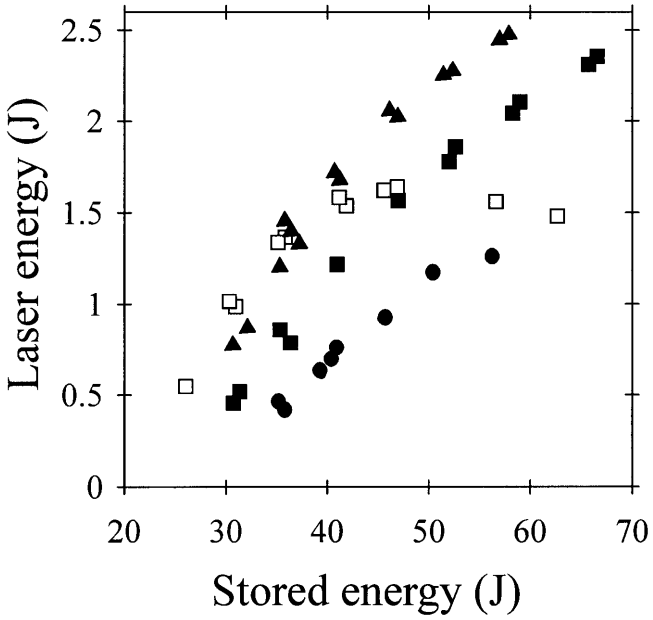

Fig. 10. Laser energy plotted against the initially stored electrical energy, for mixtures with ethane at $C = 144$ nF. Ethane partial pressure: (□)2 Torr, (▲)7.5 Torr, (■)15 Torr, (●)22 Torr

than those achieved with hydrogen owing to the very different behaviour of the discharge in H_2 and C_2H_6 mixtures. For ethane, the enhancement of E_{trans}, through the increase of C, leads to the enhancement of E_L, except at a very low pressure. In that way the best performance with ethane, $E_L = 3$ J at an efficiency $\eta = 4.7\%$, is obtained at $C = 144$ nF for the X525 laser [18]. It corresponds to a maximum specific output energy equal to 9.6 J/l.

Results obtained at 2 Torr in Fig. 10 are particular. Indeed, a concentration of at least 3% of ethane in the mixture is necessary to induce the discharge stabilization at $C = 144$ nF. This minimum concentration value is higher than at $C = 72$ nF, so that the stabilization effect by ethane should be correlated to the values of the parameters involved in the instability onset in Ne/SF_6. Discharge instabilities induce a decrease of E_L and η when E_{sto} increases at a low ethane concentration. However, at $p_{RH} = 2$ Torr and $C = 144$ nF, the laser maximum energy is about 1 J higher than the energy obtained with the H_2 mixture at the same p_{RH} and C values. This is explained by the shorter delay time, for ethane, of the laser peak power with respect to the time of the peak current, owing to a higher rate constant for the formation of the HF molecule [26].

At p_{RH} higher than 2 Torr, the evolution of E_L with respect to E_{sto} and p_{RH} at $C = 144$ nF are qualitatively identical to those obtained at 72 nF, Fig. 4. This is also the case for the efficiency. The laser energy and the efficiency are lower for the C_2H_6 mixture than for the H_2 mixture at a high p_{RH} value, 22 Torr, as already established at 72 nF and explained by the decrease of the total F-atom density produced in the discharge [21]. On the other hand, at a given ethane pressure value, the maximum efficiency at 144 nF is lower than the efficiency at 72 nF. This is mainly due to a decrease of the intrinsic efficiency, η_{int}, as the transmitted energy increases with the capacitance value.

4 Conclusions

A detailed experimental study of an X-ray photo-triggered HF laser has been performed in $Ne/SF_6/H_2$ and $Ne/SF_6/C_2H_6$ mixtures. Main characteristics of this laser, X525, are an active volume of 312 cm^3, an inter-electrode gap of 2.5 cm, and a profiled cathode. High laser performance has been achieved using ethane: an output energy of 3 J corresponding to a specific energy of 9.6 J/l at an electrical efficiency of 4.7%. Compared with previous studies [14, 15], it confirms that the active volume of the photo-triggered HF laser can be increased without loss of performance. In particular, the photo-triggering technique has allowed us to achieve the highest efficiency reported to date.

The discharge dynamics have been examined through current and voltage measurements coupled to a spatially and temporally resolved diagnostic of the plasma fluorescence intensity in the inter-electrode space. These measurements have been performed together with the measure, in absolute values, of the laser energetic characteristics, i.e. the temporal evolution of the laser power, the laser energy, and the electrical efficiency. As a result the correlations between, on the one hand, the discharge-pumped HF-laser performances which are achieved with SF_6 and hydrogen or with SF_6 and ethane, and, on the other hand, the discharge dynamics, are precisely determined for the first time. Parameters involved in this study have been the storage line capacitance and the circuit inductance, the capacitors' charging voltage, the RH-molecule type and partial pressure.

For a homogeneous active medium, the laser energy E_L and the efficiency η achieved with the mixture that contains hydrogen is quasi-identical to the performance achieved with ethane, at a low RH partial pressure value. For both mixtures, E_L increases when the electrical charge and energy transmitted to the active medium, Q_{trans} and E_{trans}, increase. On the other hand the increase of the RH pressure leads to lower E_L and η values in the case of ethane, compared to the performance obtained with hydrogen. These results are correlated to the F-atom production kinetics as already shown for a small active volume laser (50 cm^3), X510 [21]. Studies on both the X510 and X525 lasers emphasise that the transmitted energy and charge do not depend on the RH-molecule type in the range of RH pressure values usually used for HF lasers. However the spatial quality of the discharge depends very much on that molecule as soon as Q_{trans} and E_{trans} increase above critical values.

For the mixture with hydrogen, the specific laser energy and the efficiency cannot be enhanced above 5.75 J/l and 3.5% respectively, by the increase of Q_{trans} and E_{trans} through either the increase of the charging voltage or of the capacitance. These maximum laser performance values are clear consequences of the onset of discharge instabilities, which lead to the development of strong plasma inhomogeneities in the inter-electrode space at the time of the laser emission. Moreover instabilities are characteristics of the discharge in the Ne/SF_6 mixture, and the presence of hydrogen has little effect on the discharge behaviour. However the H_2-pressure value takes a prominent part in the optimization of the laser performance, as the time delay between the laser emission growth and the development of plasma inhomogeneities depends very much on that pressure.

In contrast, a stable and homogeneous discharge has been obtained over a large range of C_2H_6 pressure, charging voltage, and capacitance values when ethane is added to Ne/SF_6. As a result, the transmission efficiency in the $Ne/SF_6/C_2H_6$ can be readily optimized up to 100% by the increase of the charging voltage, whatever the circuit configuration is, with the condition that the ethane concentration in the mixture is equal to or higher than 3%. It implies that the laser energy can be readily enhanced by the increase of the capacitance value in order to increase the transmitted charge and energy to the active medium. However the overall efficiency saturates and slightly decreases at high Q_{trans} and E_{trans} values, owing to the decrease of the intrinsic efficiency of the medium.

Finally, as the most important result, it has been unambiguously demonstrated for the first time that the highest discharge-pumped HF laser performance achieved with a heavy hydrocarbon, i.e. ethane in the present work, with respect to performance achieved with hydrogen, follow from the stabilization of the discharge in SF_6 by addition of this hydrocarbon.

Acknowledgements. The authors wish to thank the DSP/STTC (DGA) for its financial support through contract No. 93/34092.

References

1. T. Deutsch: Appl. Phys. Lett. **10**, 234 (1967)
2. T. Jacobson, G. Kimbell: J. Appl. Phys. **42**, 3402 (1971)
3. R. Wenzel, G. Arnold: IEEE J. Quantum Electron. **QE-8**, 26 (1972)
4. T. Jacobson, G. Kimbell: IEEE J. Quantum Electron. **QE-9**, 173 (1973)
5. H. Pummer, W. Breitfeld, H. Wedler, G. Klement, K. Kompa: Appl. Phys. Lett. **22**, 319 (1973)
6. C. Wiswall, D. Ames, T. Menne: IEEE J. Quantum Electron. **QE-9**, 181 (1973), and references therein
7. F. Voignier, M. Gastaud: Appl. Phys. Lett. **25**, 649 (1974)
8. S. Suchard, J. Airey: *Handbook of Chemical Lasers* (Wiley, New York 1976), and references therein
9. G. Wlodarczyk: IEEE J. Quantum Electron. **QE-14**, 768 (1978)
10. D. Malyuta, V. Tolstov: Sov. J. Quantum Electron. **13**, 253 (1983)
11. V. Baranov, F. Vysikaïlo, A. Dem'yanov, D. Malyuta, V. Tolstov: Sov. J. Quantum Electron. **14**, 791 (1984)
12. E. Gorton, P. Cross, E. Parcell: Opt. Commun. **70**, 245 (1989)
13. H. Brunet, M. Mabru, J. Rocca Serra, C. Vannier: Proc. SPIE **1397**, 273 (1991)
14. V. Puech, P. Prigent, H. Brunet: Appl. Phys. B **55**, 183 (1992)
15. H. Brunet, M. Mabru, F. Voignier: Proc. SPIE **2502**, 388 (1994)
16. F. Goryunov, K. Gurkov, M. Lomaev, E. Sosnin, V. Tarasenko: Quantum Electron. **24**, 1064 (1994)
17. Y. Kalisky, K. Waichman, S. Kamin, D. Chuchem: Opt. Commun. **137**, 59 (1197)
18. F. Doussiet, M. Legentil, S. Pasquiers, C. Postel, V. Puech, L. Richeboeuf: Proc. SPIE **2702**, 179 (1996)
19. L. Richeboeuf, F. Doussiet, M. Legentil, S. Pasquiers, C. Postel, V. Puech: Proc. SPIE **2788**, 84 (1996)
20. N. Anderson, T. Bearpak, S. Scott: Appl. Phys. B **63**, 565 (1996)
21. L. Richebeouf, S. Pasquiers, M. Legentil, V. Puech: J. Phys. D **31**, 373 (1998)
22. R. Riva, M. Legentil, S. Pasquiers, V. Puech: J. Phys. D **26**, 1061 (1993)
23. S. Pasquiers, M-C. Bordage, M. Legentil, V. Puech, R. Riva, P. Ségur: Ann. Phys. **19**(C1), 213 (1994)
24. R. Riva, M. Legentil, S. Pasquiers, V. Puech: J. Phys. D **28**, 856 (1995)
25. S. Leone: J. Phys. Chem. Ref. Data **11**, 953 (1992)
26. D. Smith, D. Setser, K. Kim, D. Bogan: J. Phys. Chem. **81**, 898 (1977)